JACS JOURNAL OF THE AMERICAN CHEMICAL SOCIETY

Communication

Cite This: J. Am. Chem. Soc. 2019, 141, 17498−17502

pubs.acs.org/JACS

Reversible and Selective Interconversion of Hydrogen and Carbon Dioxide into Formate by a Semiartificial Formate Hydrogenlyase Mimic

Katarzyna P. Sokol,[†,∥] William E. Robinson,[†,∥] Ana R. Oliveira,[‡] Sonia Zacarias,[‡] Chong-Yong Lee,[†] Christopher Madden,[†] Arnau Bassegoda,[§] Judy Hirst,[§] Inês A. C. Pereira,[‡] and Erwin Reisner*[,†]

[†]Department of Chemistry, University of Cambridge, Lensfield Road, Cambridge CB2 1EW, U.K.

[‡]Instituto de Tecnologia Química e Biológica António Xavier (ITQB), Universidade NOVA de Lisboa, Av. da República, 2780-157 Oeiras, Portugal

[§]Medical Research Council Mitochondrial Biology Unit, University of Cambridge, The Keith Peters Building, Cambridge Biomedical Campus, Hills Road, Cambridge CB2 0XY, U.K.

Supporting Information

ABSTRACT: The biological formate hydrogenlyase (FHL) complex links a formate dehydrogenase (FDH) to a hydrogenase (H_2ase) and produces H_2 and CO_2 from formate via mixed-acid fermentation in *Escherichia coli*. Here, we describe an electrochemical and a colloidal semiartificial FHL system that consists of an FDH and a H_2ase immobilized on conductive indium tin oxide (ITO) as an electron relay. These *in vitro* systems benefit from the efficient wiring of a highly active enzyme pair and allow for the reversible conversion of formate to H_2 and CO_2 under ambient temperature and pressure. The hybrid systems provide a template for the design of synthetic catalysts and surpass the FHL complex *in vivo* by storing and releasing H_2 on demand by interconverting CO_2/H_2 and formate with minimal bias in either direction.

Semiartificial catalytic systems combine synthetic and biological units to drive challenging reactions and provide new concepts for catalyst design.[1] Such solar-driven systems have already demonstrated coupling of water oxidation to the reduction of CO_2,[2−4] and protons[4,5] for the production of chemical fuels. However, storage and transport of energy vectors are also important components in energy production−utilization cycles and their development will benefit from more advanced approaches and model systems.

H_2 is a promising fuel in a carbon-neutral economy and its conversion to formate allows for easier storage and transport. H_2 and formate are therefore an attractive energy vector pair. Furthermore, H_2 gas cleanly separates from dissolved formate, and their interconversion comes at little thermodynamic cost (eqs 1−3).[6,7] Achieving kinetic efficiency in HCO_2^-/H_2 interconversion remains a synthetic challenge. Artificial systems commonly compete between decomposition of formic acid to CO and H_2O (dehydration), and CO_2 and H_2 (dehydrogenation), and rely on precious metals, high temperature/pressure, organic solvents, and light.[8−10]

$$CO_2 + H^+ \rightleftharpoons HCO_2^- \ (E^{\circ\prime} = -0.366 \text{ V vs SHE, pH 6.5}) \quad (1)$$

$$2H^+ \rightleftharpoons H_2 \ (E^{\circ\prime} = -0.382 \text{ V vs SHE, pH 6.5}) \quad (2)$$

$$HCO_2^- + H^+ \rightleftharpoons CO_2 + H_2 \ (E^{\circ\prime}_{rxn} = U^{\circ\prime} = -0.016 \text{ V}) \quad (3)$$

FHL complexes are biological machines for HCO_2^-/H_2 interconversion.[11] They are either membrane-associated complexes composed of a multisubunit [NiFe]-H_2ase coupled to an FDH,[11−13] or smaller soluble complexes of an [FeFe]-H_2ase and an FDH.[14,15] The *E. coli* FHL-1 complex, composed of the membrane-bound [NiFe]-H_2ase 3 (HYD-3/HycE) and FDH-H (FdhF; Figure 1a), represents a well-studied FHL, evolving H_2 under fermentative conditions.[11,12] The constituent enzymatic units of FHL-1 have been demonstrated to be reversible electrocatalysts,[16−20] but the complex is catalytically biased toward H_2 production from formate.[14,15,19] Interconversion of HCO_2^-/H_2 has also been reported in whole-cell studies,[14,20] notably in sulfate-reducing bacteria in the absence of sulfate.[21,22] *Desulfovibrio vulgaris* Hildenborough can grow by converting formate to H_2,[23] with formate oxidation catalyzed by a periplasmic FDH, and H_2 produced either via direct (periplasmic H_2ase) or transmembrane electron transfer (cytoplasmic H_2ase).[24]

Redox biocatalysts, including H_2ases and FDHs, have been coupled to other enzymatic processes via electron relays. H_2ases have been connected to nitrate and fumarate reductases,[25] diaphorase moieties,[26] nicotinamide reductase, and alcohol dehydrogenase[27] via graphitic particles. Notably, coupling a H_2ase to carbon monoxide dehydrogenase efficiently catalyzed the water−gas shift reaction.[28] Enzymatic cascades have linked FDH with formaldehyde and alcohol dehydrogenases for methanol production.[29,30] However, the reversible interconversion of substrate and product has not been previously accomplished with such coupled enzymes *in vitro*.

Here, a semiartificial FHL complex mimic is presented by rewiring FDH[31,32] and H_2ase[33] from *D. vulgaris* Hildenborough into electrochemical and colloidal systems (Figure

Received: September 4, 2019
Published: October 22, 2019

DOI: 10.1021/jacs.9b09575
J. Am. Chem. Soc. 2019, 141, 17498−17502

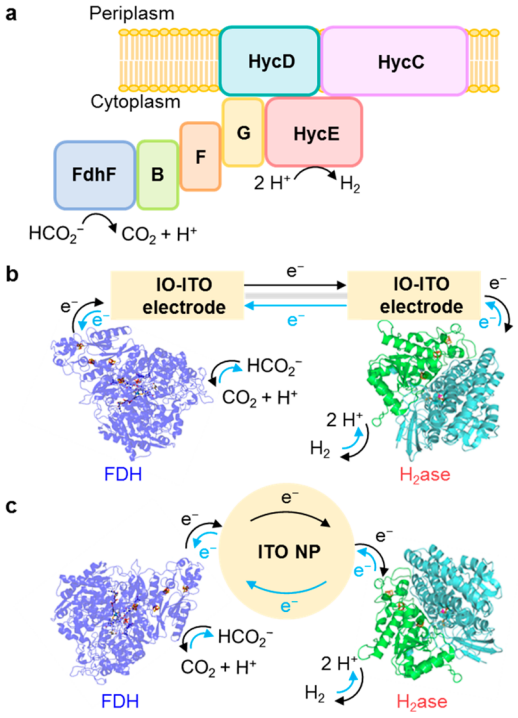

Figure 1. (a) Biological *E. coli* FHL-1 complex. FdhF, [Mo]-FDH; B/F/G, Fe−S cluster-containing proteins; HycE, [NiFe]-H_2ase; HycD/C, membrane proteins.[17] (b) IO-ITO|FDH||IO-ITO|H_2ase cell: IO-ITO|FDH wired to IO-ITO|H_2ase electrode. (c) FDH−ITO−H_2ase nanoparticle (NP) system with enzymes immobilized onto ITO NP in solution. Species size not drawn to scale.

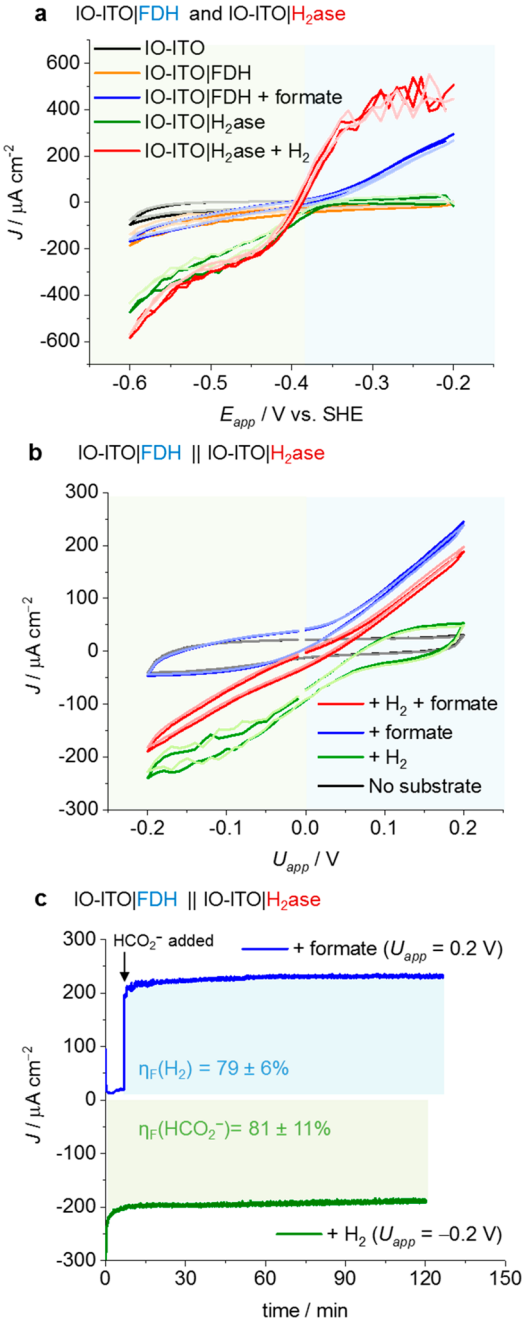

Figure 2. (a) Three-electrode PFV (ν = 5 mV s^{-1}, 1st and 5th scan, increasing transparency) using IO-ITO|FDH or IO-ITO|H_2ase working, Ag/AgCl (KCl_{sat}) reference and Pt mesh counter electrodes. (b) Two-electrode PFV (ν = 5 mV s^{-1}, 1st and 5th scan) of IO-ITO|FDH wired to IO-ITO|H_2ase. (c) Two-electrode CPE of IO-ITO|FDH wired to IO-ITO|H_2ase. Conditions: CO_2/$NaHCO_3$ (100 mM), KCl (50 mM), 1 bar CO_2 or 0.4/0.6 bar H_2/CO_2, $pH_{initial}$ = 6.5−6.7, T = 25 °C, stirring. Substrates: formate (20 mM) and/or 0.4/0.6 bar H_2/CO_2.

1b,c). These systems rely on efficient electrical contact of the [W/Se]-FDH active site via four [Fe_4S_4] clusters and the [NiFeSe]-H_2ase active-site via three [Fe_4S_4] clusters with nanostructured ITO.

Macro-mesoporous inverse opal (IO) ITO electrodes (20 μm film thickness; 0.25 cm^2 geometrical surface area) were assembled as previously reported.[34] IO-ITO|FDH and IO-ITO|H_2ase electrodes were prepared by drop-casting an FDH solution (2 μL, 19 μM with 50 mM DL-dithiothreitol, incubated for 15 min) and a H_2ase solution (2 μL, 5 μM), onto IO-ITO.[31,34] Protein film voltammetry (PFV) was recorded using a three-electrode configuration (Figures 2a and S1) in CO_2/$NaHCO_3$ solution. Current densities (J) of −185 μA cm^{-2} (CO_2 reduction to formate by FDH) and −450 μA cm^{-2} (H^+ reduction to H_2 by H_2ase) were observed at an applied potential (E_{app}) of −0.6 V vs standard hydrogen electrode (SHE). Addition of sodium formate (20 mM) to the IO-ITO|FDH system resulted in formate oxidation to CO_2, and 300 μA cm^{-2} was reached at −0.2 V vs SHE. After purging the IO-ITO|H_2ase system with H_2 (0.4 bar), H_2 oxidation to H^+ was observed and 440 μA cm^{-2} was reached at −0.2 V vs SHE. The voltammograms cut through zero current around the formal potentials of the CO_2/HCO_2^- (eq 1) and H^+/H_2 redox couples (eq 2), demonstrating reversible electrocatalysis for both enzymes.[6,35]

Multiple PFV scans of IO-ITO|FDH and IO-ITO|H_2ase (Figure S2) showed minimal desorption/activity losses. Controlled-potential electrolysis (CPE) of IO-ITO|FDH and IO-ITO|H_2ase was performed to measure H^+/CO_2 reduction (E_{app} = −0.6 V) as well as H_2/formate oxidation (E_{app} = −0.2 V) (Figure S3). Following equilibration, both electrodes retained good activity after 24 h in both directions. Faradaic efficiencies (η_F) for formate and H_2 production were determined to be 76% and 77%, respectively. Efficiency losses may be attributed to the capacitive background current of porous IO-ITO,[34] undetected trapped product, and a contribution from ITO/FTO degradation.[36,37]

The comparable formal redox potentials of H^+/H_2 and CO_2/HCO_2^- conversion (eq 1-3), reversible catalysis of the

DOI: 10.1021/jacs.9b09575
J. Am. Chem. Soc. 2019, 141, 17498−17502

individual enzymes, high and matching current densities, and good stability make this enzyme pair a promising candidate for assembling a reversible HCO_2^-/H_2 interconversion system.[6] Thus, the IO-ITO|FDH (working electrode) was wired to the IO-ITO|H_2ase (counter electrode) in a two-electrode configuration (Figure 2b). When no additional substrate was present (only buffering CO_2 and H^+), only a noncatalytic current attributed to IO-ITO capacitance was observed. Upon addition of formate, an oxidative current was observed (formate oxidation to CO_2 and H^+ reduction to H_2) at a positive applied voltage ($U > 0$ V); 250 μA cm^{-2} was reached at U = 0.2 V. Addition of H_2 resulted in a reductive current (H_2 oxidation to H^+ and CO_2 reduction to formate) at a negative voltage with −250 μA cm^{-2} obtained at U = −0.2 V.

To achieve reversible formate/H_2 interconversion (eq 3) both formate and H_2 were added in addition to CO_2 and H^+. A reversible voltammogram was observed, with zero current at approximately $U^{\circ\prime}$ at 0.02 V. A marginally more positive or negative voltage drove the reaction in either direction, demonstrating reversible unbiased electrocatalysis. 200 μA cm^{-2} and −200 μA cm^{-2} were reached at U = 0.2 V and −0.2 V, respectively. Multiple PFV scans of the IO-ITO|FDH||IO-ITO|H_2ase cell (Figure S4) showed stability of the system with marginal losses. Control experiments with IO-ITO|FDH (or ITO|H_2ase) wired to IO-ITO (Figure S5) gave only a small capacitive current in the presence and absence of substrates (H_2/formate).

CPE over 2 h at U_{app} = 0.2 V with the IO-ITO|FDH||IO-ITO|H_2ase cell with formate present (Figure 2c) produced H_2 (5.84 ± 0.88 μmol cm^{-2}) with η_F of (79 ± 11)%. Similarly, CPE at U_{app} = −0.2 V for 2 h with H_2 present generated formate (5.00 ± 0.80 μmol cm^{-2}) with η_F of (81 ± 15)%. This semiartificial electrochemical FHL system exhibited good stability, retaining >95% of its initial activity after 2 h in both directions. After equilibration, the cell exhibited high bidirectional stability for >1 day (Figure S6). For formate oxidation (U_{app} = 0.2 V), H_2 (36.28 μmol cm^{-2}) was detected with η_F = 72%. For H_2 oxidation (U_{app} = −0.2 V), formate (42.80 μmol cm^{-2}) was detected with η_F = 77%. Similarly to the three-electrode systems, capacitive currents and FTO/ITO dissolution[36,37] might have decreased the product yield.

To further investigate the system's reversibility without electrochemical wiring, FDH and H_2ase were coassembled on ITO nanoparticles (NPs) (0.3 mg mL^{-1}) (Figures 3 and S7) dispersed in electrolyte solution (see Supporting Information). Solutions of FDH (19 nM, incubated as above) and H_2ase (3.4 nM) were added to the vessel, which was sealed and purged with CO_2. Either formate or H_2 was introduced to the vessel. FDH:H_2ase molar ratios (Figure S8) and total concentrations (Figure S9a,b) were screened for the optimum H_2 evolution rate. The optimal system contained an enzyme loading of approximately 40 FDH and 7 H_2ase particles per ITO NP, based on the adsorption surface area of 27 m^2 g^{-1}, ~31 400 nm^2 per NP (assuming a 50 nm diameter sphere), and an enzyme footprint of ~100 nm^2.

Upon formate addition to the FDH−ITO−H_2ase system (Figure 3a), H_2 was produced with a reaction rate (Figure S9c) of 0.24 ± 0.01 μmol H_2 h^{-1} during the first 8 h [turnover number, TON = (23.0 ± 1.5) × 10^3 and turnover frequency, TOF = 6.4 ± 0.4 s^{-1} for the H_2ase], after which the rate started to decrease (Table S1). Equilibrium was reached after ~72 h (5.82 ± 0.24 μmol H_2, pH 6.88, T = 23 °C), in agreement with

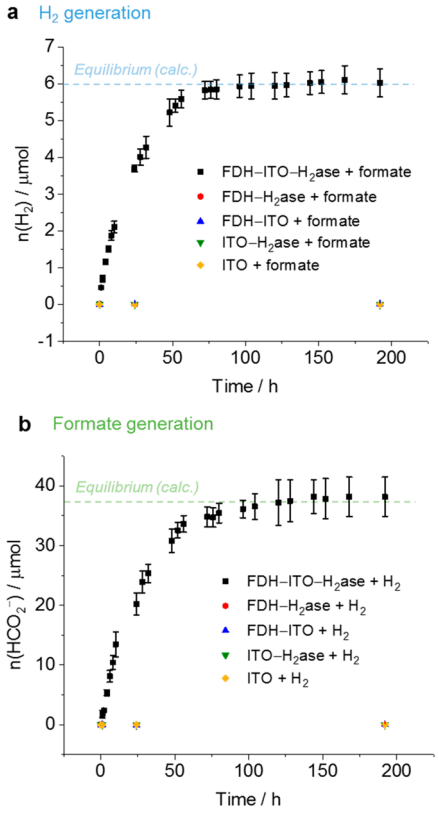

Figure 3. Product quantification of the colloidal FDH−ITO−H_2ase NP system: using ITO NPs (0.3 mg mL^{-1}), FDH (19.0 nM) and H_2ase (3.4 nM). (a) H_2 production in the presence of 10 mM formate and 1 bar CO_2. $V_{headspace}$ = 1.72 mL. (b) Formate production in the presence of 0.4/0.6 bar H_2/CO_2. $V_{solution}$ = 2 mL. Conditions: CO_2/$NaHCO_3$ (100 mM), KCl (50 mM), 1 bar CO_2 or 0.4/0.6 bar H_2/CO_2, $pH_{initial}$ = 6.5−6.7, T = 23 °C, stirring.

calculations (5.95 μmol, 2.97 mM of H_2; see Supporting Information).[7]

In the presence of H_2, the FDH−ITO−H_2ase system (Figure 3b) produced formate with an initial reaction rate of 1.33 ± 0.01 μmol formate h^{-1} [TON = (15.8 ± 5.4) × 10^3 and TOF = 4.4 ± 1.5 s^{-1} for the FDH] for the first 8 h (Figure S9d). Equilibrium was reached after ~96 h (36.16 ± 1.47 μmol formate, pH 6.99, T = 23 °C), consistent with calculations (37.11 μmol, 18.56 mM of formate).[7] Control experiments with no ITO NPs, omitting an enzyme or with denatured enzymes (Figure S10), showed only negligible H_2 and formate production (<0.2 μmol) (Tables S2 and S3). Therefore, the ITO NPs act as a semiheterogeneous electron relay facilitating electron transfer between electroactive FDH and H_2ase.

In *D. vulgaris* cells, the two periplasmic enzymes exchange electrons through the type-I cytochrome c_3 (TpIc_3) electron acceptor.[24] We therefore studied the activity of these enzymes in solution with TpIc_3. A high concentration of the cytochrome (1.9 μM, 100-fold excess vs FDH) was required to achieve comparable kinetics of H_2 and formate production (Figure S11a,b), revealing the superiority of coimmobilizing the two enzymes on synthetic ITO NPs to achieve efficient electron transfer.

In summary, we have presented how semiartificial systems consisting of FDH and H_2ase from *D. vulgaris* wired to ITO can mimic the biological FHL complex. The semiartificial FHL systems are based on a bottom-up design that employs a pair of

DOI: 10.1021/jacs.9b09575
J. Am. Chem. Soc. 2019, 141, 17498−17502

reversible redox enzymes immobilized on conductive scaffolds to enable an overall catalytic reaction to proceed to thermodynamic equilibrium. The semiartificial FHL concept can be deployed in either an electrochemical cell or a self-assembled colloidal suspension, providing versatility for applications in different contexts. The design concept of linking two half-reactions via a conductive scaffold also provides a blueprint to develop improved synthetic H_2/formate cycling catalysts in future development.

■ ASSOCIATED CONTENT

Supporting Information

The Supporting Information is available free of charge on the ACS Publications website at DOI: 10.1021/jacs.9b09575.

Materials, experimental methods, figures and tables (PDF)

■ AUTHOR INFORMATION

Corresponding Author

*reisner@ch.cam.ac.uk

ORCID

Judy Hirst: 0000-0001-8667-6797

Erwin Reisner: 0000-0002-7781-1616

Author Contributions

‖K.P.S. and W.E.R. contributed equally.

Notes

The authors declare no competing financial interest.

Additional data related to this publication are available at the University of Cambridge data repository (https://doi.org/10.17863/CAM.45156).

■ ACKNOWLEDGMENTS

This work was supported by ERC Consolidator Grant "MatEnSAP" (682833), BBSRC (BB/J000124/1, BB/I026367/1), EPSRC (EP/L015978/1, EP/G037221/1, nanoDTC and a DTA studentship to K.P.S.), a Marie Curie IntraEuropean Fellowship (PIEF-GA-2013-625034), a Fundação para a Ciência e Tecnologia (Portugal) fellowship SFRH/BD/116515/2016, Grants PTDC/BIA-MIC/2723/2014, PTDC/BBB-BEP/2885/2014, R&D units UID/Multi/04551/2013 (Green-IT) and LISBOA-01-0145-FEDER-007660 (MostMicro), cofunded by FCT/MCTES and FEDER funds through COMPETE2020/POCI, and European Union's Horizon 2020 (No. 810856).

■ REFERENCES

(1) Kornienko, N.; Zhang, J. Z.; Sakimoto, K. K.; Yang, P.; Reisner, E. Interfacing Nature's Catalytic Machinery with Synthetic Materials for Semi-Artificial Photosynthesis. *Nat. Nanotechnol.* **2018**, *13*, 890–899.

(2) Woolerton, T. W.; Sheard, S.; Reisner, E.; Pierce, E.; Ragsdale, S. W.; Armstrong, F. A. Efficient and Clean Photoreduction of CO_2 to CO by Enzyme-Modified TiO_2 Nanoparticles Using Visible Light. *J. Am. Chem. Soc.* **2010**, *132*, 2132–2133.

(3) Liu, C.; Gallagher, J. J.; Sakimoto, K. K.; Nichols, E. M.; Chang, C. J.; Chang, M. C. Y.; Yang, P. Nanowire-Bacteria Hybrids for Unassisted Solar Carbon Dioxide Fixation to Value-Added Chemicals. *Nano Lett.* **2015**, *15*, 3634–3639.

(4) Sokol, K. P.; Robinson, W. E.; Warnan, J.; Kornienko, N.; Nowaczyk, M. M.; Ruff, A.; Zhang, J. Z.; Reisner, E. Bias-Free Photoelectrochemical Water Splitting with Photosystem II on a Dye-Sensitized Photoanode Wired to Hydrogenase. *Nat. Energy* **2018**, *3*, 944–951.

(5) Brown, K. A.; Wilker, M. B.; Boehm, M.; Dukovic, G.; King, P. W. Characterization of Photochemical Processes for H_2 Production by CdS Nanorod-[FeFe] Hydrogenase Complexes. *J. Am. Chem. Soc.* **2012**, *134*, 5627–5636.

(6) Armstrong, F. A.; Hirst, J. Reversibility and Efficiency in Electrocatalytic Energy Conversion and Lessons from Enzymes. *Proc. Natl. Acad. Sci. U. S. A.* **2011**, *108*, 14049–14054.

(7) Reda, T.; Plugge, C. M.; Abram, N. J.; Hirst, J. Reversible Interconversion of Carbon Dioxide and Formate by an Electroactive Enzyme. *Proc. Natl. Acad. Sci. U. S. A.* **2008**, *105*, 10654–10658.

(8) Loges, B.; Boddien, A.; Junge, H.; Beller, M. Controlled Generation of Hydrogen from Formic Acid Amine Adducts at Room Temperature and Application in H_2/O_2 Fuel Cells. *Angew. Chem., Int. Ed.* **2008**, *47*, 3962–3965.

(9) Kuehnel, M. F.; Wakerley, D. W.; Orchard, K. L.; Reisner, E. Photocatalytic Formic Acid Conversion on CdS Nanocrystals with Controllable Selectivity for H_2 or CO. *Angew. Chem., Int. Ed.* **2015**, *54*, 9627–9631.

(10) Sordakis, K.; Tang, C.; Vogt, L. K.; Junge, H.; Dyson, P. J.; Beller, M. Homogeneous Catalysis for Sustainable Hydrogen Storage in Formic Acid and Alcohols. *Chem. Rev.* **2018**, *118*, 372–433.

(11) Finney, A. J.; Sargent, F. *Advances in Microbial Physiology*; Academic Press: London, 2019; Vol. *74*.

(12) Pinske, C. *Advances in Microbial Physiology*; Academic Press: London, 2019; Vol. *74*.

(13) Lim, J. K.; Mayer, F.; Kang, S. G.; Müller, V. Energy Conservation by Oxidation of Formate to Carbon Dioxide and Hydrogen via a Sodium Ion Current in a Hyperthermophilic Archaeon. *Proc. Natl. Acad. Sci. U. S. A.* **2014**, *111*, 11497–11502.

(14) Schuchmann, K.; Müller, V. Direct and Reversible Hydrogenation of CO_2 to Formate by a Bacterial Carbon Dioxide Reductase. *Science* **2013**, *342*, 1382–1386.

(15) Schwarz, F. M.; Schuchmann, K.; Müller, V. Hydrogenation of CO_2 at Ambient Pressure Catalyzed by a Highly Active Thermostable Biocatalyst. *Biotechnol. Biofuels* **2018**, *11*, 237.

(16) Bassegoda, A.; Madden, C.; Wakerley, D. W.; Reisner, E.; Hirst, J. Reversible Interconversion of CO_2 and Formate by a Molybdenum-Containing Formate Dehydrogenase. *J. Am. Chem. Soc.* **2014**, *136*, 15473–15476.

(17) McDowall, J. S.; Murphy, B. J.; Haumann, M.; Palmer, T.; Armstrong, F. A.; Sargent, F. Bacterial Formate Hydrogenlyase Complex. *Proc. Natl. Acad. Sci. U. S. A.* **2014**, *111*, E3948–E3956.

(18) Mcdowall, J. S.; Hjersing, M. C.; Palmer, T.; Sargent, F. Dissection and Engineering of the Escherichia Coli Formate Hydrogenlyase Complex. *FEBS Lett.* **2015**, *589*, 3141–3147.

(19) Pinske, C.; Sargent, F. Exploring the Directionality of Escherichia Coli Formate Hydrogenlyase: A Membrane-Bound Enzyme Capable of Fixing Carbon Dioxide to Organic Acid. *MicrobiologyOpen* **2016**, *5*, 721–737.

(20) Roger, M.; Brown, F.; Gabrielli, W.; Sargent, F. Efficient Hydrogen-Dependent Carbon Dioxide Reduction by Escherichia Coli. *Curr. Biol.* **2018**, *28*, 140–145.

(21) da Silva, S. M.; Voordouw, J.; Leitão, C.; Martins, M.; Voordouw, G.; Pereira, I. A. C. Function of Formate Dehydrogenases in Desulfovibrio Vulgaris Hildenborough Energy Metabolism. *Microbiology* **2013**, *159*, 1760–1769.

(22) Mourato, C.; Martins, M.; da Silva, S. M.; Pereira, I. A. C. A Continuous System for Biocatalytic Hydrogenation of CO_2 to Formate. *Bioresour. Technol.* **2017**, *235*, 149–156.

(23) Martins, M.; Mourato, C.; Pereira, I. A. C. Desulfovibrio Vulgaris Growth Coupled to Formate-Driven H_2 Production. *Environ. Sci. Technol.* **2015**, *49*, 14655–14662.

(24) Martins, M.; Mourato, C.; Morais-Silva, F. O.; Rodrigues-Pousada, C.; Voordouw, G.; Wall, J. D.; Pereira, I. A. C. Electron Transfer Pathways of Formate-Driven H_2 Production in Desulfovibrio. *Appl. Microbiol. Biotechnol.* **2016**, *100*, 8135–8146.

(25) Vincent, K. A.; Li, X.; Blanford, C. F.; Belsey, N. A.; Weiner, J. H.; Armstrong, F. A. Enzymatic Catalysis on Conducting Graphite Particles. *Nat. Chem. Biol.* **2007**, *3*, 761–762.

(26) Reeve, H. A.; Lauterbach, L.; Ash, P. A.; Lenz, O.; Vincent, K. A. A Modular System for Regeneration of NAD Cofactors Using Graphite Particles Modified with Hydrogenase and Diaphorase Moieties. *Chem. Commun.* **2012**, *48*, 1589−1591.
(27) Reeve, H. A.; Lauterbach, L.; Lenz, O.; Vincent, K. A. Enzyme-Modified Particles for Selective Biocatalytic Hydrogenation by Hydrogen-Driven NADH Recycling. *ChemCatChem* **2015**, *7*, 3480−3487.
(28) Lazarus, O.; Woolerton, T. W.; Parkin, A.; Lukey, M. J.; Reisner, E.; Seravalli, J.; Pierce, E.; Ragsdale, S. W.; Sargent, F.; Armstrong, F. A. Water-Gas Shift Reaction Catalyzed by Redox Enzymes on Conducting Graphite Platelets. *J. Am. Chem. Soc.* **2009**, *131*, 14154−14155.
(29) Nam, D. H.; Kuk, S. K.; Choe, H.; Lee, S.; Ko, J. W.; Son, E. J.; Choi, E. G.; Kim, Y. H.; Park, C. B. Enzymatic Photosynthesis of Formate from Carbon Dioxide Coupled with Highly Efficient Photoelectrochemical Regeneration of Nicotinamide Cofactors. *Green Chem.* **2016**, *18*, 5989−5993.
(30) Kuk, S. K.; Singh, R. K.; Nam, D. H.; Singh, R.; Lee, J. K.; Park, C. B. Photoelectrochemical Reduction of Carbon Dioxide to Methanol through a Highly Efficient Enzyme Cascade. *Angew. Chem., Int. Ed.* **2017**, *56*, 3827−3832.
(31) Sokol, K. P.; Robinson, W. E.; Oliveira, A. R.; Warnan, J.; Nowaczyk, M. M.; Ruff, A.; Pereira, A. C.; Reisner, E. Photoreduction of CO_2 with a Formate Dehydrogenase Driven by Photosystem II Using a Semi-Artificial Z-Scheme Architecture. *J. Am. Chem. Soc.* **2018**, *140*, 16418−16422.
(32) Miller, M.; Robinson, W. E.; Oliveira, A. R.; Heidary, N.; Kornienko, N.; Warnan, J.; Pereira, I. A. C.; Reisner, E. Interfacing Formate Dehydrogenase with Metal Oxides for the Reversible Electrocatalysis and Solar-Driven Reduction of Carbon Dioxide. *Angew. Chem., Int. Ed.* **2019**, *58*, 4601−4605.
(33) Marques, M. C.; Tapia, C.; Gutiérrez-Sanz, O.; Ramos, A. R.; Keller, K. L.; Wall, J. D.; De Lacey, A. L.; Matias, P. M.; Pereira, I. A. C. The Direct Role of Selenocysteine in [NiFeSe] Hydrogenase Maturation and Catalysis. *Nat. Chem. Biol.* **2017**, *13*, 544−550.
(34) Mersch, D.; Lee, C.-Y.; Zhang, J. Z.; Brinkert, K.; Fontecilla-Camps, J. C.; Rutherford, A. W.; Reisner, E. Wiring of Photosystem II to Hydrogenase for Photoelectrochemical Water-Splitting. *J. Am. Chem. Soc.* **2015**, *137*, 8541−8549.
(35) Léger, C.; Bertrand, P. Direct Electrochemistry of Redox Enzymes as a Tool for Mechanistic Studies Direct Electrochemistry of Redox Enzymes as a Tool for Mechanistic Studies. *Chem. Rev.* **2008**, *108*, 2379−2438.
(36) Benck, J. D.; Pinaud, B. A.; Gorlin, Y.; Jaramillo, T. F. Substrate Selection for Fundamental Studies of Electrocatalysts and Photoelectrodes: Inert Potential Windows in Acidic, Neutral, and Basic Electrolyte. *PLoS One* **2014**, *9*, e107942.
(37) Geiger, S.; Kasian, O.; Mingers, A. M.; Mayrhofer, K. J. J.; Cherevko, S. Stability Limits of Tin-Based Electrocatalyst Supports. *Sci. Rep.* **2017**, *7*, 3−9.

DOI: 10.1021/jacs.9b09575
J. Am. Chem. Soc. 2019, 141, 17498−17502